Poly-L-Arginine Predominantly Increases the Paracellular Permeability of Hydrophilic Macromolecules across Rabbit Nasal Epithelium *in Vitro*

Kazuo Ohtake,[1] Takuya Maeno,[1] Hideo Ueda,[1] Hideshi Natsume,[1,2] and Yasunori Morimoto[1,2,3]

Received July 8, 2002; accepted October 22, 2002

Purpose. The purpose of this work was to characterize the main transport pathway of hydrophilic macromolecules induced by poly-L-arginine (poly-L-Arg; molecular weight 42.4 kDa) across the excised rabbit nasal epithelium.

Methods. Excised rabbit nasal epithelium was mounted in an Ussing-type chamber for measurement of fluorescein isothiocyanate-labeled dextran (FD-4; molecular weight 4.4 kDa) transport and transepithelial electrical resistance (TEER). The main transport pathway of FD-4 enhanced by poly-L-Arg was evaluated using confocal laser scanning microscopy. Immunolocalization of junction proteins (ZO-1, occludin, and E-cadherin) after treatment with poly-L-Arg was also observed.

Results. After apical application of a poly-L-Arg (0.05, 0.5, and 5 mg/mL), the permeability coefficient of FD-4 increased by 1.6-, 2.9-, and 5.2-fold, respectively, compared with the control of $5.2 \pm 1.3 \times 10^{-7}$ cm/s. Consistent with the increase in transport, there was a concurrent reduction in TEER. At a concentration of 0.05 mg/mL poly-L-Arg, both FD-4 transport and TEER returned to the control level. A good correlation was obtained between the FD-4 permeability coefficient and 1/TEER. Basolateral application of poly-L-Arg at 5 mg/mL, however, did not increase FD-4 transport. Marked FD-4 fluorescence was located in the paracellular spaces after treatment with apical poly-L-Arg compared with that in the absence of poly-L-Arg. Immunofluorescence of ZO-1, occludin, and E-cadherin in cell-to-cell junctions was reduced and distributed into the cytoplasm by apical application of poly-L-Arg, suggesting that poly-L-Arg regulates the junction proteins to enhance paracellular permeability across the nasal epithelium. After pretreatment with either 2,4-dinitrophenol or ouabain, the enhancing effect of apical poly-L-Arg was abolished, indicating the contribution of metabolic energy (cell viability) to the poly-L-Arg-mediated enhancing effect.

Conclusion. In the nasal epithelium, apical poly-L-Arg appears to increase predominantly the paracellular transport of hydrophilic macromolecules via disorganization of tight- and adherens-junction proteins. The regulatory mechanism of the poly-L-Arg effect is likely to be dependent on energy-requiring cellular processes.

KEY WORDS: poly-L-arginine; hydrophilic macromolecules; tight junctions; paracellular permeability; nasal epithelium.

INTRODUCTION

The potential for using the nose as an alternative route for administering water-soluble drugs, in particular biologically active peptides and proteins, has attracted considerable interest in recent years because of the higher absorption and permeability of active drugs through the nasal epithelia compared with other mucosae (1,2). However, because of the inherent low bioavailability resulting from the insufficiently permeable nature and mucociliary clearance of nasal epithelia, there has been interest in developing a specific delivery formulation containing absorption-enhancing agents and/or mucoadhesive materials (3–6). Unfortunately, most chemical enhancers (surfactants, bile salts, fatty acids, etc.) induce irreversible damage and irritate the nasal mucosa when used at concentrations that provide adequate absorption of peptide and protein drugs (7,8).

Recently, it has been shown that polycationic materials, such as poly-L-arginine (poly-L-Arg; 9,10), poly-L-lysine (9,10), protamine (11), chitosan (12–14), and *N*-trimethyl chitosan (15) have the potential to promote the transmucosal delivery of macromolecules without severe epithelial toxicity, and so are ideal for drug transport through nasal epithelium. Natsume *et al.* have reported that poly-L-Arg of different molecular weights (MW) can enhance the *in vivo* nasal absorption of fluorescein isothiocyanate-labeled dextran (FD-4; MW 4.4 kDa), a model hydrophilic compound in rats, without severe toxicity to the excised rabbit nasal epithelia (16). The enhancing effect of poly-L-Arg is dependent of their concentration and MW as well as the charge density of an individual poly-L-Arg molecule (17). Poly-L-Arg exhibits MW-dependent transient and reversible effects on the enhancement of FD-4 absorption in rats, associated with the rate of degradation of poly-L-arginine by the peptidase in the nasal mucus (18). In addition, under confocal laser scanning microscopy (CLSM), it has been shown that poly-L-Arg enhances FD-4 absorption mainly via the paracellular route after co-administration *in vivo* (18). Although the results obtained in these *in vivo* studies should allow increased nasal absorption of FD-4 via the poly-L-Arg-induced cellular response, which is responsible for the transient opening of cell-to-cell junctions, they provide only limited information about the mechanism of poly-L-arginine action in the nasal epithelium.

In vitro experiments (experimental techniques) using cultured cell monolayers have been used to analyze the enhancing effect of polycations while monitoring the bioelectric parameters, potential difference (PD), and short-circuit current (Isc), as well as transepithelial electrical resistance (TEER). In Madin-Darby canine kidney cell monolayers, poly-L-Arg and poly-L-lysine increase the transport of paracellular markers, such as [^{14}C]-D-mannitol and [^{3}H]-inulin, and concurrently reduce TEER after apical application (9). Moreover, the reduction in TEER occurred only after apical application and not basolateral application, suggesting a site specificity of the cellular responses to poly-L-lysine (9). Similar results in Caco-2 monolayers were reported for chitosan by Schipper *et al.* (13). These studies suggest that conformational changes in the paracellular barrier occurred as a cellular action mediated by polycations rather than as a consequence of a direct action on the junction complex (9,11,13). Thus, an *in vitro* analysis of drug transport with measurement of the bioelectric parameters in the nasal epithelium could be more helpful and informative in elucidating the possible mechanism of the increased transport achieved by poly-L-Arg involving the induction of cellular responses.

[1] Faculty of Pharmaceutical Sciences, Josai University, 1-1 Keyakidai, Sakado, Saitama 350-0295, Japan.

[2] Research Institute of TTS Technology, 1-1 Keyakidai, Sakado, Saitama 350-0295, Japan.

[3] To whom correspondence should be addressed. (e-mail: morimoto@josai.ac.jp)

0724-8741/03/0200-0153/0

The purpose of the present study was to characterize the enhancing effect of poly-L-Arg with a mean MW of 42.4 kDa on the transport of water-soluble macromolecules across the excised rabbit nasal epithelium using the Ussing chamber system *in vitro*. The transport of FD-4 and TEER was monitored to estimate the contribution of paracellular permeability to poly-L-Arg-induced absorption enhancement as well as visualizing the transport pathway by CLSM. Immunolocalization of ZO-1, a tight junction-associated protein, occludin, a transmembrane protein of the tight junction, and E-cadherin, an adherens junction protein, were observed after treatment with poly-L-Arg. Furthermore, the effect of poly-L-Arg on the nasal transport of FD-4 was measured in the presence of the metabolic inhibitors, 2,4-dinitrophenol (DNP) and ouabain, to determine the role of metabolic energy (epithelial viability) in the poly-L-Arg effect.

MATERIALS AND METHODS

Materials

FD-4, poly-L-Arg hydrochloride, and normal goat serum were purchased from Sigma Chemical Co., Ltd. (St Louis, MO, USA). Sodium taurodihydrofusidate (STDHF) was a kind gift from Leo Pharmaceuticals (Bullerup, Denmark). DNP and ouabain were obtained from Wako Pure Chemical Industries (Osaka, Japan). Mouse anti-ZO-1 monoclonal antibodies and mouse anti-occludin monoclonal antibodies were obtained from Zymed Laboratories Inc. (San Francisco, CA, USA). Rat anti-E-cadherin monoclonal antibodies were obtained from TaKaRa Shuzo Co., Ltd (Kyoto, Japan). FITC-conjugated goat affinity purified antibody to mouse IgG and rhodamine-conjugated goat affinity purified antibody to rat IgG were obtained from ICN Biomedicals (Irvine, CA, USA). All other chemicals were of reagent grade.

Preparation of Isolated Nasal Tissue

The method has been fully described by Kubo *et al.* (19). Briefly, male Japanese white rabbits (Tokyo Laboratory Animals, Tokyo, Japan), weighing 2.5–3.0 kg were sacrificed by slowly increasing the CO_2 concentration in a CO_2 gas animal euthanasia cabinet (KN-750-1, Natsume Co., Ltd, Tokyo) according to the NIH standards as described in "Principles of Laboratory Animal Care." The nasal septum was then gently removed. After trimming, the excised nasal epithelium was carefully mounted in the tissue adapter with a circular aperture of 0.5 cm^2. The adapter-tissue assembly was then placed between two halves of Ussing chambers maintained at 37 ± 1°C. The bathing solution, bicarbonate Ringer's solution (BRS, 4 mL on each side) was bubbled with 95% O_2/5% CO_2 to maintain the pH at 7.4. BRS consisted of 125 mM NaCl, 5 mM KCl, 10 mM $NaHCO_3$, 1.2 mM NaH_2PO_4, 1.4 mM $CaCl_2$, and 11 mM D-glucose.

Measurement of Bioelectric Parameters

All experiments were performed under open-circuit conditions with intermittent short-circuit conditions using a short-circuit current amplifier (CEZ-9100, Nippon Koden, Tokyo, Japan). PD was measured with two matched calomel electrodes. Two salt-agar bridges (containing 3% agar in 4 M KCl), whose tips were located near the center of the tissue surfaces, were used to connect electrically the reservoir fluids to the electrode wells (20). The electrical output of the calomel electrodes was amplified by the voltage-clamp unit. The direct current across the tissue was transmitted via a pair of matched Ag/AgCl electrodes with conducting agar bridges, with the tips positioned away from the tissue surfaces at the far ends of the reservoirs. The Isc flowing in the bath-tissue-bath current was monitored at 10-min intervals. TEER was calculated as follows: TEER = PD/(Isc × A) according to Ohm's law, where A is the effective permeation area (0.5 cm^2). Before each experiment, the solution resistance (< 100 $\Omega \cdot cm^2$) was compensated for by the automatic voltage clamp unit. A baseline PD of 6.8 ± 0.8 mV, Isc of 121 ± 17 $\mu A/cm^2$, and TEER of 56.6 ± 5.9 $\Omega \cdot cm^2$ were observed for 96 nasal mucosae, comparable with previous results (2,8,19).

Transport Study

After the bioelectric parameters (PD, Isc, and TEER) had been allowed to equilibrate for about 120 min, both the apical and basolateral bathing fluids were replaced with fresh BRS to minimize any possible degradation of poly-L-Arg in the nasal mucus (18,21). This confirmed no effect of the replacement of bathing fluids on the monitoring of the bioelectric parameters. Solute transport was initiated by replacing appropriate amounts of apical solution with BRS (pH 7.2–7.5) containing FD-4 (final concentration 2.5 mg/mL) and poly-L-Arg at various concentrations (final concentration 0.05–5 mg/mL). To evaluate the site specificity of poly-L-Arg action, 5 mg/mL poly-L-Arg and 2.5 mg/mL FD-4 were added to the basolateral side. In a separate experiment, 5 mg/mL poly-L-Arg and 2.5 mg/mL FD-4 were added to the apical and basolateral sides, respectively. An aliquot (1.0 mL) was sampled from either apical or basolateral side at 10-min intervals up to 120 min to determine the appearance of FD-4. For comparison with poly-L-Arg, similar experiments were conducted using 5 mg/mL STDHF, a synthetic bile salt derivative, as a possible chemical enhancer.

To verify the energy dependence of the nasal epithelium in which the poly-L-Arg action was being initiated, the nasal epithelium was pretreated with 1 mM DNP for 30 min on both the apical and basolateral sides or 1 mM ouabain for 30 min on the basolateral side before starting the transport experiment. At this concentration, the Isc was completely abolished in the presence of DNP on both the apical and basolateral sides and ouabain on the basolateral side, respectively, whereas increases in TEER up to ~125% were evident (data not shown). After rinsing the epithelium twice with fresh BRS, poly-L-Arg (5 mg/mL) and FD-4 (2.5 mg/mL) were added to the apical side. At predetermined time intervals, samples (1 mL) were taken from the basolateral side as described above.

FD-4 Assay

One hundred microliters of sample solution was diluted 50-fold with potassium dihydrogenphosphate-sodium borate buffer (pH 8.5). The fluorescence of FD-4 was determined in a fluorescence spectrofluorometer (RF-5000, Shimadzu, Kyoto, Japan) at an excitation wavelength of 495 nm and an emission wavelength of 515 nm.

CLSM Observation

Transport Visualization of FD-4

After the bioelectric parameters had reached equilibrium, the fluid in both chambers was replaced with fresh BRS and then poly-L-Arg (5 mg/mL) and FD-4 (2.5 mg/mL) were dissolved in BRS were added to the apical side for 120 min. Thereafter, the nasal epithelium was removed from the Ussing chamber, rinsed with phosphate-buffered saline (PBS, 13 mM NaH_2PO_4, 87 mM Na_2HPO_4, and 51 mM NaCl, pH 7.4) and fixed in 3.75% formalin-PBS for 8–10 h at room temperature. The fixed epithelium was sandwiched between a glass slide and coverslip in a 1:1 solution of PBS-glycerol and stuck on a glass slide with glue to set on the CLSM platform. The fluorescence of FD-4 in the nasal epithelium was then observed by CLSM. Because the fixed mucosal surface is not flat because of the difficulty in excising the epithelium, the CLSM pictures obtained cover various regions from the cilia to the z-axis (in depth). Hence, the confocal laser scanned sections each 3.6 μm in depth from a focusing area of the nasal epithelium in this experiment. An MRC-600 Lasersharp System (Bio-Rad Laboratories, Richmond, CA, USA), linked to a Zeiss Axioplan equipped with a Zeiss Neofluar (×63, NA 1.25 oil objective, Carl Zeiss, Oberkochen, Germany), was set for confocal imaging. The fluorescence of FD-4 was excited at an Argon laser wavelength of 488 nm. All experiments were performed in triplicate.

Immunolocalization

For ZO-1, occludin, and E-cadherin imaging, poly-L-Arg at a concentration of 0.05, 0.5 and 5 mg/mL was added to the apical side after the bioelectric parameters had stabilized. After treatment with poly-L-Arg for either 30 or 120 min, the nasal epithelium was removed from the Ussing chamber, rinsed with tris-buffered saline (TBS, 50 mM tris-HCl, pH 7.4, 150 mM NaCl) containing 10 mM $CaCl_2$ (TBS-Ca) three times for 15 min, fixed in 3.75% formalin-TBS-Ca for 10 min at room temperature, and 0.25% Triton X-100 in TBS-Ca was allowed to permeate for 50 min at room temperature. The tissue was then incubated for 30 min in 50% normal goat serum in TBS-Ca and then overnight at 4°C with the following antibodies: 1:100 mouse anti-ZO-1 monoclonal antibodies, 1:50 rat anti-E-cadherin monoclonal antibodies, and 1:100 mouse anti-occludin monoclonal antibodies in 50% normal goat serum in TBS-Ca. After rinsing in TBS-Ca 3 times for 15 min, the tissue was then incubated for 120 min with the following secondary antibodies: 1:50 FITC-conjugated goat anti-mouse IgG or 1:25 rhodamine-conjugated goat anti-rat IgG in 50% normal goat serum in TBS-Ca. After rinsing in TBS-Ca three times for 15 min, the labeled tissue was cut into small pieces (4–5 mm^2) and mounted between a glass slide and coverslip (see section Transport Visualization of FD-4). The fluorescence was excited at an argon/krypton laser wavelength of either 488 or 568 nm. A composite picture of 20 sections (0.2-μm apart on the z axis) of each membrane was collected for analysis. All experiments were performed in triplicate.

Data Analysis

The apparent permeability coefficient (P_{app}) and TEER were determined as follows in all experiments except for 0.05 mg/mL poly-L-Arg on the apical side. The P_{app} of FD-4 was calculated using the following equation:

$$P_{app}\ (cm/s) = dQ/dt \times 1/A \times C_0$$

where dQ/dt (μg/s) is the rate of appearance of FD-4 on the receiver side from 50 min to 120 min after application of FD-4 with and without poly-L-Arg, C_0 (μg/mL) is the initial FD-4 concentration on the donor side, and A (cm^2) is the effective surface area of the nasal epithelium.

The change in TEER is shown as the ratio to the baseline TEER (time = 0 min), and the average TEER was calculated from 50 to 120 min. The TEER was also converted to membrane conductance (G_t = 1/TEER) to evaluate the correlation with P_{app}. In the case of 0.05 mg/mL poly-L-Arg, because FD-4 permeation and TEER profiles vs. time after poly-L-Arg administration were non-steady state and because there was a time difference between the increased permeation and the reduction in TEER reached a maximum (see Fig. 1), the

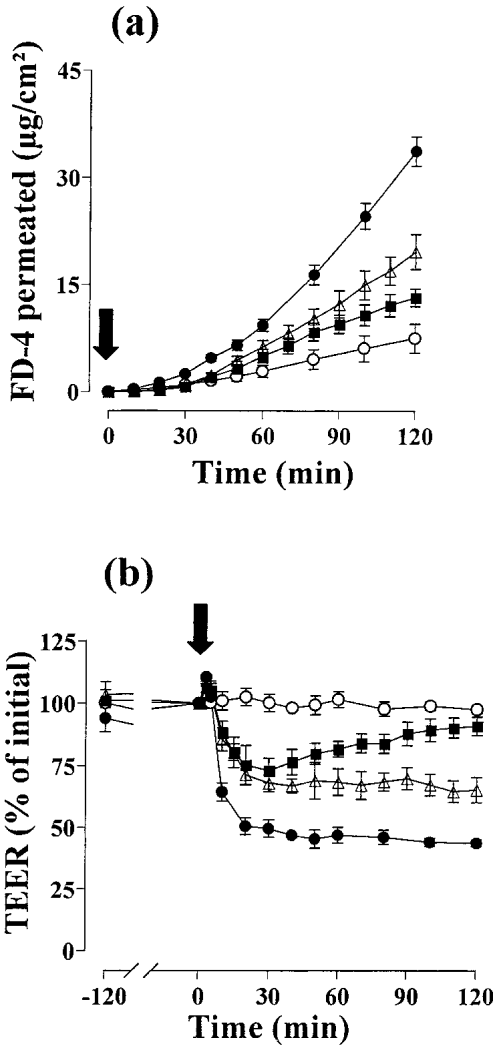

Fig. 1. Effects of poly-L-arginine (poly-L-Arg) concentration on the fluorescein isothiocyanate-labeled dextran permeation (a) and transepithelial electrical resistance (b) across the rabbit nasal epithelium. (○) control; (■) with 0.05 mg/mL poly-L-Arg; (Δ) with 0.5 mg/mL poly-L-Arg; (●) with 5 mg/mL poly-L-Arg. Filled arrow: apical application of poly-L-Arg and fluorescein isothiocyanate-labeled dextran (2.5 mg/mL). Data represent mean ± SE (n = 3–5).

values of the increase in FD-4 permeability and the reduction in TEER were calculated from 40 to 70 min and 20 to 40 min to estimate the P_{app} and TEER changes, respectively.

Statistics

Statistical analyses were performed using Student's *t* test. A p value of 0.05 was considered significant.

RESULTS

Effect of Poly-L-Arg on FD-4 Transport and TEER

Figures 1a and b show the cumulative amount of FD-4 permeated and TEER vs. time across the excised rabbit nasal epithelium after apical application of poly-L-Arg at various concentrations. FD-4 transport across the nasal epithelium was increased in a poly-L-Arg concentration-dependent manner. The P_{app} of FD-4 calculated at a poly-L-Arg concentration of 0.05, 0.5, and 5 mg/mL was 1.6-, 2.9-, and 5.2-fold the control value of $5.2 \pm 1.3 \times 10^{-7}$ cm/s, respectively. Consistent with the increase in FD-4 transport, there was a reduction in TEER (Fig. 1b). At a concentration of 0.05 mg/mL poly-L-Arg, both FD-4 transport and TEER returned to the control and baseline values 90 min after the application of poly-L-Arg (P_{app} of FD-4; $6.6 \pm 0.8 \times 10^{-7}$ cm/s and average TEER; 89.7 ± 0.7% calculated from 90 min to 120 min). The relationship between P_{app} and G_t for individual data is given in Fig. 2. A good correlation ($r^2 = 0.859$, $p < 0.0001$) was observed between P_{app} and G_t, suggesting that membrane resistance involves FD-4 permeability.

Transport Pathway of FD-4

CLSM images of the horizontal section of rabbit nasal epithelium 120 min after application of FD-4 in the presence and absence of poly-L-Arg are shown in Fig. 3. In the absence of poly-L-Arg (control), FD-4 was located partially around the nasal epithelial cells up to 7.2 μm in depth (Fig. 3a). Intracellular localization of FD-4 was also observed in some cells, but this was not clear because of the much lower fluorescence intensity in these regions. In contrast, FD-4 fluorescence around the cells was marked compared with controls up to 7.2 μm in depth in the presence of poly-L-Arg (Fig. 3b), suggesting that poly-L-Arg may open cell-to-cell junctions, increasing paracellular solute transport. As indicated by the open arrows, fluorescence was observed around the cilia. Perhaps a gel-like complex of cationic poly-L-Arg with anionic glycoproteins (e.g., sialomucin) in mucus is formed with loading FD-4, adsorbing around the cilia surface (22). Moreover, marked fluorescence around the cells appeared at a scan depth of 3.6 and 7.2 μm in these regions (indicated by open arrows).

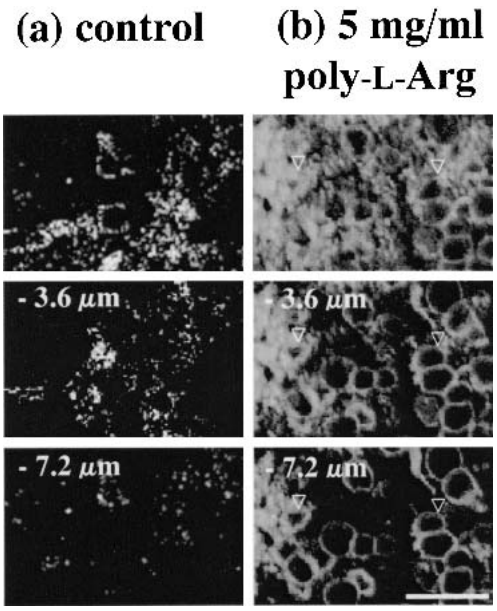

Fig. 3. Confocal laser scanning microscopy of rabbit nasal epithelium after a 120-min application of fluorescein isothiocyanate-labeled dextran (FD-4) with or without 5 mg/mL poly-L-Arg. Series of three horizontal cross-sections from 0–7.2 μm that were taken at steps of 3.6 μm in thickness. Open arrowheads: FD-4 fluorescence was seen around the cilia surface, perhaps because of the formation of a gel-like complex of cationic poly-L-Arg with anionic proteins in mucus with loading FD-4. In these regions, marked fluorescence around the cells appeared at a scan depth of 3.6 and 7.2 μm. Scale bar: 30 μm.

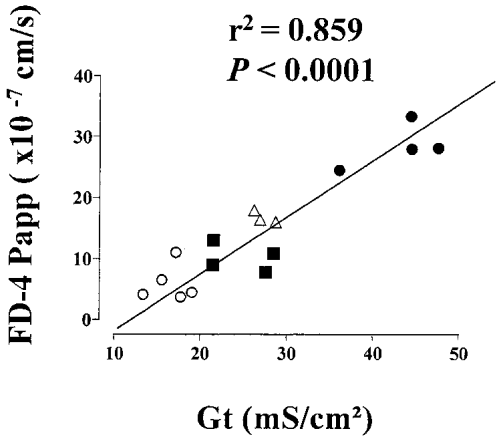

Fig. 2. Relationship between fluorescein isothiocyanate-labeled dextran P_{app} and G_t in individual data sets. (○) control: (■) with 0.05 mg/mL poly-L-arginine (poly-L-Arg); (Δ) with 0.5 mg/mL poly-L-Arg; (●) with 5 mg/mL poly-L-Arg.

Site Specificity of Poly-L-Arg Action

Table I summarizes the Papp and TEER values under various conditions after the application of poly-L-Arg and STDHF. When poly-L-Arg at 5 mg/mL was co-administered with FD-4 to the apical side, FD-4 transport in the apical-to-basolateral (A to B) direction was increased 4.8-fold with a 57% reduction in TEER compared with the control value, whereas the basolateral application of poly-L-Arg did not increase FD-4 transport in the basolateral to apical (B to A) direction. Furthermore, apical application of poly-L-Arg also increased FD-4 transport in the B to A direction, and the P_{app} and TEER values were fairly similar to those in the A to B direction. These results indicate that the enhancement of FD-4 transport by poly-L-Arg occurs only on the apical membrane, in that poly-L-Arg produces site-specific action in the excised rabbit nasal epithelium. In contrast, either apical or basolateral application of STDHF at 5 mg/mL significantly increased FD-4 transport in both directions (Table I).

Table I. Effect of Apical (A) or Basolateral (B) Application of Enhancers on P_{app} of Fluorescein Isotriocyonate-Labeled Dextra (FD-4) and Transepithelial Electrical Resistance (TEER)

Direction of FD-4 transport	Papp ($\times 10^{-7}$ cm/s)	TEER ($\Omega \cdot cm^2$)
A-to-B direction		
Control (5)	5.67 ± 1.00	55.60 ± 1.17
Apical 5 mg/mL poly-L-Arg (4)	27.13 ± 1.97* [478%]	31.42 ± 1.95* [57%]
Apical 5 mg/mL STDHF (4)	27.74 ± 2.96* [489%]	18.37 ± 4.39* [33%]
B-to-A direction		
Control (5)	6.34 ± 0.72	56.93 ± 5.83
Basolateral 5 mg/mL poly-L-Arg (5)	3.41 ± 0.83* [54%]	60.45 ± 8.42 [106%]
Apical 5 mg/mL poly-L-Arg (3)	20.05 ± 1.27* [316%]	36.52 ± 5.16* [64%]
Basolateral 5 mg/mL STDHF (4)	32.14 ± 3.63* [507%]	25.23 ± 3.11* [44%]

Note: P_{app} and average TEER were calculated from 50 min to 120 min. * $p < 0.05$ vs. control, ( ): n, [ ]: ratio to control, Data represent the mean ± SE.

Effect of Poly-L-Arg on Localization of ZO-1, Occludin, and E-cadherin

Figure 4 shows the immunofluorescent CLSM images of the rabbit nasal epithelium for ZO-1, occludin, and E-cadherin. In control epithelium (without poly-L-Arg), these proteins were clearly localized in the cell-to-cell contact region on the plasma membrane (Fig. 4a-c). After exposure to poly-L-Arg at a concentration of 0.5 and 5 mg/mL for 120 min, immunofluorescence staining for ZO-1, occludin, and E-cadherin in the cell-to-cell contact region appeared to be reduced and distributed inside the cells (Fig. 4j-o). As expected from the TEER recovery at 0.05 mg/mL poly-L-Arg (Fig. 1b, ■), these proteins had distributed inside the cells at 30 min (Fig. 4d-f), and then the greater part was recovered at 120 min at this concentration (Fig. 4g-i). However, basolateral application of poly-L-Arg at a concentration of 5 mg/mL for 120 min had no effect on immunostaining for these proteins compared with the control (Fig. 4p-r). These results suggest that the increased permeation of FD-4 corresponding with the reduced TEER after apical application of poly-L-Arg is possibly caused by disorganization of junction proteins in the cell-to-cell contact region.

Effect of DNP and Ouabain on FD-4 Transport

The effect of DNP and ouabain on poly-L-Arg- and STDHF-induced FD-4 transport in the A to B direction is shown in Fig. 5. Pretreatment with 1 mM DNP and ouabain did not affect the P_{app} of FD-4 compared with the control. After pretreatment with DNP and ouabain, the enhancing effect of poly-L-Arg on FD-4 transport was completely abolished (Fig. 5), whereas TEER was reduced by 14 and 39%, respectively (data not shown). However, STDHF at 5 mg/mL significantly increased FD-4 transport regardless of the absence of metabolic energy provided by DNP and ouabain.

DISCUSSION

In the present study, we characterized the predominant transport pathway of macromolecules enhanced by poly-L-Arg in the excised rabbit nasal epithelium using an *in vitro* Ussing chamber technique. The effect of poly-L-Arg on the enhanced transport was also determined in terms of the site specificity and energy dependence (cell viability) of the nasal epithelium.

Apical application of poly-L-Arg up to 5 mg/mL resulted in a dose-dependent increase in the permeability of FD-4 (Fig. 1a), which correlated well ($r^2 = 0.859$) with G_t (Fig. 2). Several studies have shown an increase in the permeability of paracellular markers and a concurrent reduction in TEER (i.e., increase in G_t) induced by polycations in cultured cell monolayers (9,13,15). There was also a linear relationship between membrane permeability and G_t, which can be used to indicate the paracellular transport of solutes. Thus, our results show that poly-L-Arg most likely enhances the paracellular permeability of FD-4 in the excised rabbit nasal epithelium. This confirmed visualization of the transport pathway using CLSM where this technique has proven a useful tool to elucidate transport pathways via mucosal tissue (13). In the absence of poly-L-Arg, a slight fluorescence of FD-4 was observed around the cells up to 7.2 μm in depth (Fig. 3a), whereas marked fluorescence was located in the paracellular space up to 7.2 μm in the presence of poly-L-Arg (Fig. 3b). These results indicate that the transport of FD-4 enhanced by poly-L-Arg is predominantly via the paracellular pathway, and is likely to alter the nature of the cell-to-cell junctions.

Because the paracellular permeability of the solute is restricted by junction protein complexes, including ZO-1 (23) and occludin (24), it is interesting to see whether poly-L-Arg affects such proteins. We evaluated the immunofluorescent localization of ZO-1 and occludin after treatment of the excised nasal epithelium with poly-L-Arg. ZO-1 (225 kDa) and occludin (65 kDa) were identified at the tight junctions in a variety of epithelia (23–25). Without poly-L-Arg (control), both ZO-1 and occludin were present in the cellular periphery and appeared as a continuous band localized at the intercellular borders (Fig. 4a and b). The adherens junction protein, E-cadherin, was also located in the cell-to-cell contact regions (Fig. 4c). However, after exposure to poly-L-Arg on the apical side at a concentration of 0.05 for 30 min and 0.5 and 5 mg/mL for 120 min, respectively, the immunofluorescence of ZO-1, occludin, and E-cadherin in the cell-to-cell contact region appeared to be reduced and distributed inside the cells (Fig. 4d-f and j-o). At a lower concentration of poly-L-Arg, some immunofluorescence of junction proteins was still present around the cells (Fig. 4g-i). Thus, it is evident that poly-L-Arg induces alterations in the localization of junction proteins, particularly tight junction proteins, in a poly-L-Arg concentration-dependent manner in the nasal epithelium. Overall, it was concluded that poly-L-Arg triggered the opening of tight junctions involving the intracellular distribution of junction proteins, thereby allowing predominantly paracellular transport of FD-4.

It has been shown that a reduction in TEER induced by poly-L-lysine and chitosan, respectively, occurred only after the apical application of these polycations in Madin-Darby canine kidney and Caco-2 cells, respectively (9,13). In the present study, we determined the site-specific effect of poly-L-Arg in the nasal epithelium. FD-4 permeability in both the A to B and B to A directions was increased after the apical application of poly-L-Arg at 5 mg/mL, whereas basolateral

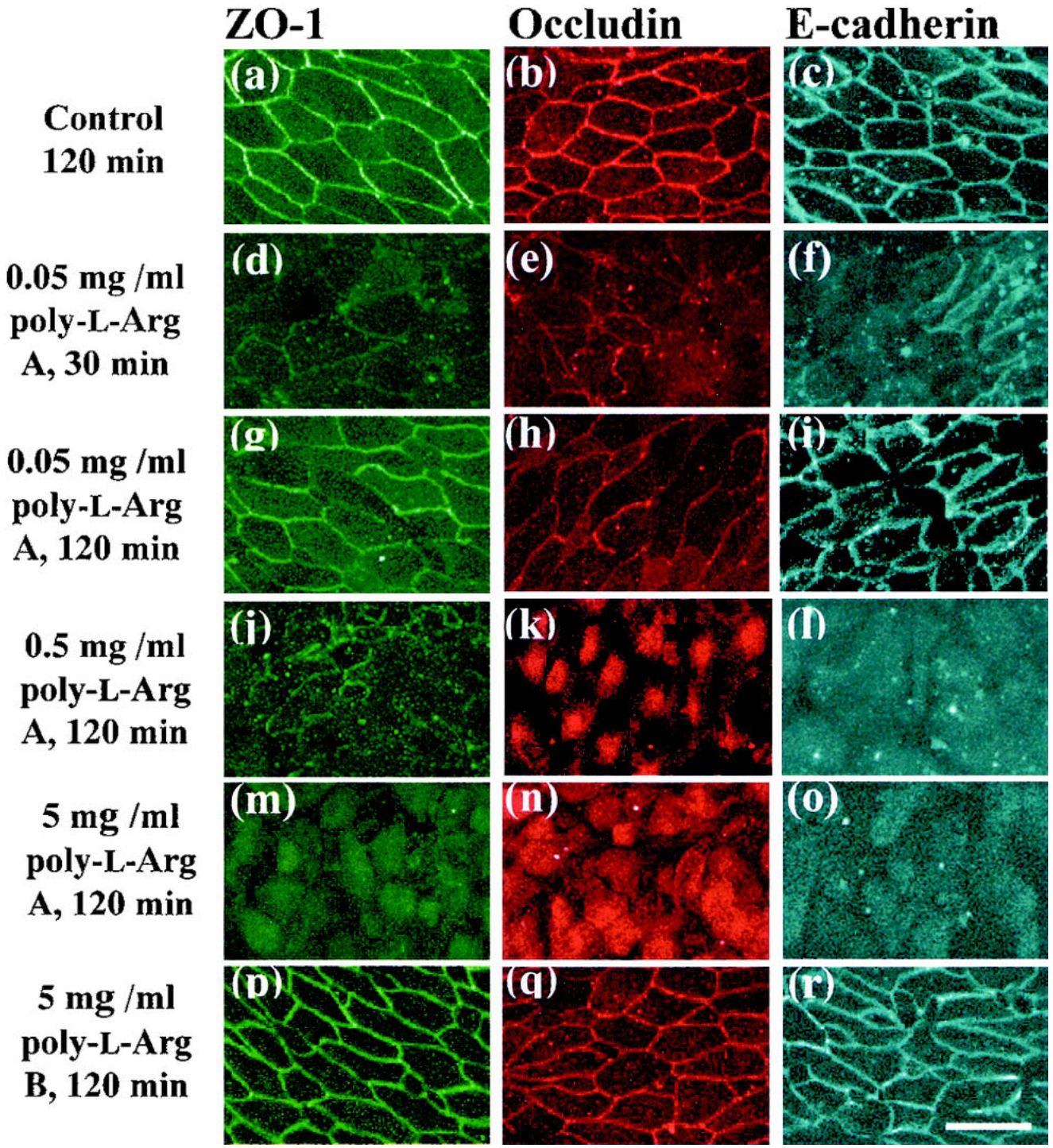

Fig. 4. Immunofluorescent localization of ZO-1 (a, d, g, j, m, and p), occludin (b, e, h, k, n, and q), and E-cadherin (c, f, i, l, o, and r) in rabbit nasal epithelium after treatment with poly-L-arginine (poly-L-Arg) under various conditions. A: apical application of poly-L-Arg. B: basolateral application of poly-L-Arg. Scale bar: 15 μm.

application had no effect on FD-4 transport in the B to A direction (Table I). No site-specific effect was observed after exposure to 5 mg/mL STDHF, which produced an enhancing effect closely associated with cell damage (7,8,16,18). In addition, the localization of ZO-1 and occludin was unaffected after the basolateral application of poly-L-Arg at 5 mg/mL for 120 min (Fig. 4p and q). Also, almost no alteration in localization of E-cadherin was observed (Fig. 4r). These results support no direct action of poly-L-Arg on junction proteins after apical application. If poly-L-Arg acts directly on junction proteins, it allows the distribution of E-cadherin inside the cells after basolateral application. Hence, poly-L-Arg was found to act only on apical membrane components, such as lipids, proteins, polysaccharides, but not on basolateral ones, in the rabbit nasal epithelium.

Although in the earlier study the candidate molecules

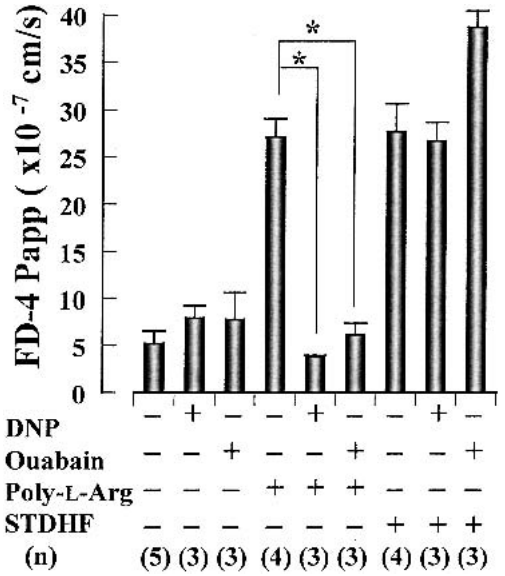

Fig. 5. Effects of DNP (1 mM) and ouabain (1 mM) on increased FD-4 permeation induced by poly-L-Arg and STDHF across rabbit nasal epithelium. There was a significant difference between the poly-L-Arg-induced increase in FD-4 P_{app} pretreatment with and without metabolic inhibitors (Student *t* test, *$p < 0.05$). Data represent mean ± SE.

specifically interacting with polycations in the nasal epithelium were not identified, removal of chitosan from the apical bathing medium after a pretreatment for 20 min did not alter the effect of cationic chitosan on apical cell membrane permeability and tight junction integrity, whereas the addition of anionic heparin after pretreatment with chitosan significantly reduced these effects (13). This suggests that electrostatic interactions between polycations, and glycoproteins in mucus and certain anionic sites on the epithelial surface may alter the charge density in the surface region, subsequently initiating cellular events. Such possible events include internalization of polycations (11), interaction with the transmembrane sialoglycoprotein podocalyxin (26), and affinity for Ca^{2+} sensing receptors (27) on various epithelia. Further studies are required to identify the specific molecules that interact with poly-L-Arg in the nasal epithelial membrane.

Several reports have shown that polycations, such as protamine and chitosan, are able to induce a reversible opening of tight junctions in different epithelial cell models (11,13,14). In the present study, the maximal FD-4 transport and concurrent reduction in TEER obtained at 30 min after apical application of 0.05 mg/mL poly-L-Arg fully recovered within 120 min (Fig. 1a and b). Additional observations of the immunolocalization of ZO-1, occludin, and E-cadherin that dispersed into cytoplasm at 30 min (Fig. 4d-f) and relocalized to the cell-to-cell contact region (Fig. 4g-i) strongly support the reversible enhancing effect of 0.05 mg/mL poly-L-Arg. However, in the removal of poly-L-Arg at 30 min after application of poly-L-Arg, TEER recovered by 80% in 0.5 mg/mL poly-L-Arg but not in 5 mg/mL poly-L-Arg (data not shown). In our previous report, 5 mg/mL poly-L-Arg has been shown to produce almost no cellular damage as far as the release of membrane components is concerned (16). Moreover, histopathological alterations in rat nasal epithelium were negligible after intranasal administration of 10 mg/mL poly-L-Arg *in vivo* (17). Furthermore, the enhancing effect of 10 mg/mL poly-L-Arg on the nasal absorption of FD-4 has been shown to be transient and reversible (18). Poly-L-Arg at a concentration up to 5 mg/mL can induce reversible changes in tight junctions *in vivo* (18), although TEER is reduced after the application of 5 mg/mL poly-L-Arg *in vitro* in this experiment. Thus, poly-L-Arg is expected to induce reversible changes in tight junctions.

We performed further studies to help us understand the relationship between poly-L-Arg action and cellular events. The possible role of metabolic energy in the poly-L-Arg-induced increase in nasal epithelial permeability was examined. The enhancing effect of poly-L-Arg was significantly inhibited in the presence of either 1 mM DNP or 1mM ouabain (Fig. 5), suggesting that the poly-L-Arg-induced increase in paracellular permeability of macromolecules is regulated by metabolic energy (cell viability) and energy-dependent cellular events may have occurred. This was supported by the observation that STDHF produced an increase in FD-4 permeation in both the presence and absence of metabolic inhibitor (Fig. 5) where enhancing effect of STDHF had been associated with cell damage (7,8,16,18). Recently, it has been shown that the localization of ZO-1 and occludin are regulated by both tyrosine (28) and serine/threonine (29) phosphorylation mechanisms which are considered to require metabolic energy. In fact, poly-L-Arg and poly-L-lysine have been shown to activate insulin receptor kinase (30), casein kinase II (31), and protein kinase C (32) in various cell types. Therefore, the initial event involving poly-L-Arg and the epithelial surface may lead to a possible final event in which poly-L-Arg-mediated disorganization of junction proteins may occur via the energy-related phosphorylation of these proteins. Unfortunately, in the presence of ouabain, poly-L-Arg led to significant reduction in TEER regardless of no enhancement of FD-4 permeation. One possible reason for this is that poly-L-Arg may induce other cellular regulatory processes, such as active ion transport (33) and cell volume regulation (34) in Na^+-K^+-ATPase-inhibited cells. Perhaps, these processes result in a change in epithelial ion conductivity, but not macromolecule transport, thereby reducing the TEER. Thus, it seems likely that poly-L-Arg regulates various types of cellular events, in particular reduction in barrier function between adjacent epithelial cells. We intend to conduct further studies of the cellular events to clarify the systematic mechanism of the poly-L-Arg effect.

In conclusion, poly-L-Arg predominantly enhances paracellular solute transport involving alteration in the localization of junction proteins, including ZO-1, occludin, and E-cadherin, in excised rabbit nasal epithelium, and acts only on the apical membrane components. The regulatory mechanism of the poly-L-Arg effect is likely to be dependent on energy-requiring cellular processes. Further investigations are necessary to clarify the mechanism of polycation-modulated junction effects in the nasal epithelium to develop a transnasal drug delivery system for macromolecules, including bioactive peptides, hormones, vaccines, and genes using polycations.

ACKNOWLEDGMENT

This work was supported in part by the Japan Science and Technology Corporation.

REFFRENCES

1. Y. W. Chien, K. S. Su, and S. Chang. *Nasal Systemic Drug Delivery*. Marcel Dekker, New York, 1989.
2. K. Hosoya, H. Kubo, H. Natsume, K. Sugibayashi, Y. Morimoto, and S. Yamashita. The structural barrier of absorptive mucosae: site difference of the permeability of fluorescein isothiocyanate-labeled dextran in rabbit. *Biopharm. Drug Dispos.* **14**:685–696 (1993).
3. C. McMartin, L. E. F. Hutchinson, R. Hyde, and G. E. Peters. Analysis of structural requirements for the absorption of drug and macromolecules from nasal cavity. *J. Pharm. Sci.* **76**:535–540 (1987).
4. K. Morimoto, H. Yamaguchi, Y. Iwakura, K. Morisaki, Y. Ohashi, and Y. Nakai. Effects of viscous hyaluronate-sodium solutions on the nasal absorption of vasopressin and an analogue. *Pharm. Res.* **8**:471–474 (1991).
5. T. Yamamoto, Y. Maitani, T. Ando, K. Isawa, K. Takayama, and T. Nagai. High absorbency and subchronic morphologic effects on the nasal epithelium of a nasal insulin powder dosage form with a soybean-derived sterlglucoside mixture in rabbit. *Biol. Pharm. Bull.* **21**:866–870 (1998).
6. R. J. Soane, M. Frier, A. C. Perkins, N. S. Jones, S. S. Davis, and L. Illum. Evaluation of the clearance characteristics of bioadhesive systems in human. *Int. J. Pharm.* **178**:55–65 (1999).
7. F. M. H. M. Merkus, N. G. M. Schipper, W. A. J. J. Hermens, V. S. G. Romeijin, and J. C. Verhoef. Absorption enhancers in nasal drug delivery: Efficacy and safety. *J. Control. Release* **24**:201–208 (1993).
8. K. Hosoya, H. Kubo, H. Natsume, K. Sugibayashi, and Y. Morimoto. Evaluation of enhancers to increase nasal absorption using Ussing chamber technique. *Biol. Pharm. Bull.* **17**:316–322 (1994).
9. G. T. A. McEwan, M. A. Jepson, B. H. Hirst, and N. L. Simmons. Polycation-induced enhancement of epithelial paracellular permeability in independent of tight junctional characteristics. *Biochem. Biophys. Acta* **1148**:51–60 (1993).
10. D. A. Uchida, C. G. Ballowe, and G. R. Cott. Cationic proteins increase the permeability of cultured rabbit tracheal epithelial cells: modification by heparin and extracellular calcium. *Exp. Lung Res.* **22**:85–99 (1996).
11. M. Hammes and A. Singh. Effect of polycations on permeability of glomerular epithelial cell monolayers to albumin. *J. Lab. Clin. Med.* **123**:437–446 (1994).
12. L. Illum, N. F. Farrai, and S. S. Davis. Chitosan as a novel delivery system for peptide drugs. *Pharm. Res.* **11**:1186–1189 (1994).
13. N. G. M. Schipper, S. Olsson, J. A. Hoogstraate, A. G. de Boer, and K. M. Varum. Chitosans as absorption enhancers for poorly absorbable drugs 2: Mechanism of absorption enhancement. *Pharm. Res.* **14**:923–929 (1997).
14. V. Dodane, M. A. Khan, and J. R. Merwin. Effect of chitosan on epithelial permeability and structure. *Int. J. Pharm.* **182**:21–32 (1999).
15. A. F. Kotze, H. L. Lueβen, B. J. Leeuw, A. G. de Boer, J. C. Verhoef. and H. E. Junjinger. *N*-trimethyl chitosan chloride as a potential absorption enhancer across mucosal surfaces: *in vitro* evaluation in intestinal epithelial cells (Caco-2). *Pharm. Res.* **14**: 1197–1202 (1997).
16. H. Natsume, S. Iwata, K. Ohtake, M. Miyamato, M. Yamaguchi, K. Hosoya, D. Kobayashi, K. Sugibayashi, and Y. Morimoto. Screening of cationic compounds as an absorption enhancer for nasal drug delivery. *Int. J. Pharm.* **185**:1–12 (1999).
17. M. Miyamoto, H. Natsume, S. Iwata, K. Ohtake, M. Yamaguchi, D. Kobayashi, K. Sugibayashi, M. Yamashina, and Y. Morimoto. Improved nasal absorption of drug using poly-L-arginine: effect of concentration and molecular weight of poly-L-arginine on the nasal absorption of FITC-dextran in rats. *Eur. J. Pharm. Biopharm.* **52**:21–30 (2001).
18. K. Ohtake, H. Natsume, H. Ueda, and Y. Morimoto. Analysis of transient and reversible effects of poly-L-arginine on the in vivo nasal absorption of FITC-dextran in rats. *J. Control. Release* **82**: 263–275 (2002).
19. H. Kubo, K. Hosoya, H. Natsume, K. Sugibayashi, and Y. Morimoto. In vitro permeation of several model drugs across rabbit nasal mucosa. *Int. J. Pharm.* **103**:27–36 (1994).
20. Y. Horibe, K. Hosoya, K. J. Kim, T. Ogiso, and V. H. Lee. Polar solute transport across the pigmented rabbit conjunctiva: size dependence and the influence of 8-bromo cyclic adenosine monophosphate. *Pharm. Res.* **14**:1246–1251 (1997).
21. K. Fukuda, K. Itoh, and T. Ooyama. A protease inhibitor from human allergic nasal secretions. *Acta Otolaryngol.* **104**:539–544 (1987).
22. R. Larochelle and B. Martineau-Doizu. Distribution and histochemical characterization of goblet cells in the nasal cavity of piglets. *Acta Otolaryngol.* **191**:103–111 (1991).
23. B. R. Stevenson, J. D. Siliciano, M. S. Mooseker, and D. A. Goodenough. Identification of ZO-1: a high molecular weigh polypeptide associated with tight junction (zonula occludens) in a variety of epithelia. *J. Cell Biol.* **103**:755–765 (1986).
24. M. Furuse, T. Hirase, M. Itoh, A. Nagafuchi, S. Yonemura, S. Tsukita, and S. Tsukita. Occludin: a novel integral membrane protein localizing at tight junctions. *J. Cell Biol.* **123**:1777–1788 (1993).
25. B. M. Denker and S. K. Nigam. Molecular structure and assembly of tight junction. *Am. J. Physiol.* **274**:F1–F9 (1998).
26. F. Pugliese, P. Mene, and G. A. Cinotti. Glomerular polyanion and controlled cell function. *Am. J. Nephrol.* **10**:14–18 (1990).
27. L. Gama, L. M. Baxendale-Cox, and C. E. Breitwiesser. Ca^{2+}-sensing receptors in intestinal epithelium. *Am. J. Physiol.* **273**:C1168–C1175 (1997).
28. T. Tsukamoto and S. Nigam. Role of tyrosine phosphorylation in the reassembly of occludin and other tight junction proteins. *Am. J. Physiol.* **276**:F737–F750 (1999).
29. A. Sakakibara, M. Furuse, M. Saitou, Y. Ando-Akatsuka, and S. Tsukita. Possible involvement of phosphorylation of occludin in tight junction formation. *J. Cell Biol.* **137**:1393–1401 (1997).
30. Y. Biener and Y. Zich. Basic polycations activate the insulin receptor kinase and a tightly associated serine kinase. *Eur. J. Biochem.* **194**:243–250 (1990).
31. D. B. Sacks and J. M. McDonald. Effects of cationic polypeptides on the activity, substrate interaction, and autophosphorylation of casein kinase II: a study with calmodulin. *Arch. Biochem. Biophys.* **299**:275–280 (1992).
32. P. S. Leventhal and P. J. Bertics. Activation of protein kinase C by selecting binding of arginine-rich polypeptides. *J. Biol. Chem.* **268**:13906–13913 (1993).
33. M. Ropke, S. Carstens, M. Haklm, and O. Frederiksen. Ion transport mechanisms in native rabbit nasal airway epithelium. *Am. J. Physiol.* **271**:L637–L645 (1996).
34. M. A. Linshaw. Effect of metabolic inhibitors on renal tubule cell volume. *Am. J. Physiol.* **239**:F571–F577 (1980).